*J. Fluid Mech.* (2001), *vol.* 437, *pp.* 395–411. Printed in the United Kingdom



# Accelerated diffusion in the centre of a vortex

By KONRAD BAJER[1], ANDREW P. BASSOM[2] AND ANDREW D. GILBERT[2]

[1]Institute of Geophysics, Warsaw University, Poland

[2]School of Mathematical Sciences, University of Exeter, Exeter EX4 4QE, UK

(Received 3 May 2000 and in revised form 31 August 2000)

The spiral wind-up and diffusive decay of a passive scalar in circular streamlines is considered. An accelerated diffusion mechanism operates to destroy scalar fluctuations on a time scale of order $P^{1/3}$ times the turn-over time, where $P$ is a Péclet number. The mechanism relies on differential rotation, that is, a non-zero gradient of angular velocity. However if the flow is smooth, the gradient of angular velocity necessarily vanishes at the centre of the streamlines, and the time scale becomes greater. The behaviour at the centre is analysed and it is found that scalar there is only destroyed on a time scale of order $P^{1/2}$. Related results are obtained for magnetic field and for weak vorticity, a scalar coupled to the stream function of the flow. Some exact solutions are presented.

## 1. Introduction

The problem of how fluid motion interacts with molecular diffusion to accelerate diffusion and transport has many facets and many applications. The aim of this paper is to clarify fundamental issues of time scales in the basic situation in which a scalar is transported in a smooth steady vortex, consisting of closed circular streamlines in planar flow. The evolution of a passive scalar in this configuration is discussed by Rhines & Young (1983) and in a similar Cartesian geometry by Moffatt (1983). These authors show that variation of structure along streamlines is destroyed on a rapid, order-$P^{1/3}$ time scale because of the action of differential rotation in enhancing gradients. Here $P$ is a Péclet number and units are chosen to make the turn-over time of the flow of order unity. Left behind is an axisymmetric distribution of scalar, constant along streamlines, which diffuses only on the longer, order-$P$ time scale of molecular diffusion.

In a related paper Moffatt & Kamkar (1983) obtain the analogous result for flux expulsion of a weak magnetic field. Here a vector potential for the magnetic field is transported as a passive scalar. The effect of accelerated diffusion is to destroy gradients of the scalar and so to expel flux from the vortex. The time scale here is of order ${R_m}^{1/3}$, where $R_m$ is the magnetic Reynolds number. These results explain the scalings found in numerical simulations of flux expulsion by Weiss (1966).

A third area in which accelerated diffusion in closed streamlines is important is the evolution of vorticity itself. In two-dimensional flow, vorticity is an active scalar as it is inextricably coupled to the stream function of the flow field. However when vorticity is weak and fine-scaled it acts approximately as a passive scalar and is often subject to spiral wind-up and accelerated diffusion. This is seen in the homogenization

of vorticity in ocean gyres (Rhines & Young 1982) and other geophysical vortices (e.g. McCalpin 1987; Sutyrin 1989; Smith & Montgomery 1995), and generally in the relaxation of flows to Prandtl–Batchelor states in which vorticity is constant along streamlines (Batchelor 1956). The time scale of accelerated diffusion is now of order $R^{1/3}$, where $R$ is the Reynolds number (Lundgren 1982). Similar time scales have been identified for viscous effects in critical-layer cat's eyes (Stewartson 1978).

These processes are important in the behaviour of coherent vortices evolving freely in two-dimensional turbulence; in this case the leading effect on the internal dynamics of a coherent vortex is a time-dependent strain from other vortices (see Lingevitch & Bernoff 1995). This can generate spiral arms of vorticity with azimuthal wavenumber $n = 2$ which are subject to accelerated diffusion as the vortex regains axisymmetry through spiral wind-up (e.g. Melander, McWilliams & Zabusky 1987; Bernoff & Lingevitch 1994) or relaxes to a state controlled by the external strain (Jiménez, Moffatt & Vasco 1996). Sometimes the vortex does not relax to axisymmetry, but after external forcing relaxes to a stable non-axisymmetric state, for example a tripole (Koumoutsakos 1997; Rossi, Lingevitch & Bernoff 1997; Dritschel 1998). This relaxation process again involves wind-up of fluctuations in vorticity, but in the streamlines of the new non-axisymmetric state, and these fluctuations would be destroyed diffusively on an order-$R^{1/3}$ time scale. For strictly inviscid flow, $R = \infty$, fluctuations always remain, but tend to zero in a coarse-grained sense (see Bassom & Gilbert 1998, referred to herein as BG, 1999, 2000).

This accelerated diffusion of an advected field in closed streamlines has been termed the 'shear–diffuse mechanism' (Bernoff & Lingevitch 1994) to emphasize the role of shear by differential rotation to enhance gradients and so diffusion. If differential rotation vanishes at a given radius, then the arguments leading to the 1/3-power-law time scale do not apply, as many authors have pointed out. However in a smooth vortex with circular streamlines, the differential rotation *necessarily* vanishes at the centre, by smoothness considerations. This raises the question we shall address in this paper: what is the time scale for accelerated diffusion of advected fields at the centre of circular streamlines, and what is the ultimate form of those fields?

To be more specific, let $\alpha(r)$ be the angular velocity of the flow, in the plane, as a function of radius $r$. If the flow is smooth, that is infinitely differentiable, then the axisymmetric stream function and vorticity distribution expand as power series in $r^2$ at the origin. The same is true for the angular velocity $\alpha(r)$ and so necessarily $\alpha'(0) = 0$. Using the linearity of the advection–diffusion equation and axisymmetry of the underlying flow, we may decompose a passive scalar field into Fourier modes proportional to $\mathrm{e}^{\mathrm{i}n\theta}$, where $n$ is an azimuthal wavenumber. For $n \neq 0$ this scalar field is wound up into spiral arms by the flow and is damped by diffusion, leading to multiplication by the damping term $\exp(-n^2\alpha'(r)^2t^3/3P)$ at a given radius $r$. The cubic power in $t$ leads to accelerated diffusion that strikes when $t = O(P^{1/3})$ for $n \neq 0$. However this assumes that $\alpha'(r) = O(1)$, and if this is not the case then a more careful estimate of the shear–diffuse time scale is

$$t_{\text{shear}-\text{diffuse}} = \alpha'(r)^{-2/3}P^{1/3} \tag{1.1}$$

(and analogously for magnetic field or vorticity). Clearly this estimate breaks down at the centre of the vortex where $\alpha'(r) = 0$, and the time scale becomes longer. Our aim is to find this longer time scale, assuming that $\alpha(r)$ has a leading quadratic behaviour in $r$ as $r \to 0$, which is the generic case for a smooth vortex.

Note that the $n = 0$ mode is unaffected by motion and is governed by just the diffusion equation; this mode decays on the long $O(P)$ time scale. We are interested

in non-axisymmetric modes with $n \neq 0$ and their accelerated decay, in other words in the relaxation of a scalar (or other) field to axisymmetry. We emphasize that our study does not apply to accelerated diffusion in a singular flow field, for example a point vortex, for which $\alpha'(r)$ diverges as $r$ tends to zero (Bajer 1998). Note also that if $\alpha'(r)$ has a wide variation with $r$ then the above estimate gives a range of time scales and this can introduce anomalous scaling properties for diffusion (Flohr & Vassilicos 1997).

The paper is structured as follows. In § 2 we consider a passive scalar in a given flow with circular streamlines and an exactly quadratic angular velocity profile $\alpha(r)$. This problem may be solved analytically for arbitrary Péclet number. The solution shows how scalar is destroyed by the shear–diffuse mechanism and reveals the new scalings for destruction of passive scalar at the origin, in particular the longer time scale there. We consider the general case of passive scalar in smooth flows with circular stream lines (§ 3). The problem becomes reduced to an inner problem close to the origin, which is identical to the exact problem discussed in § 2. We relate this to flux expulsion in § 4, and ask the question: in flux expulsion from circular streamlines how does the magnetic field at the centre of the streamlines decay (Weiss 1966)?

We consider the shear–diffuse mechanism acting on weak vorticity fluctuations (§ 5) and obtain an exact solution including viscosity, which builds on the studies of Lundgren (1982) and BG. This solution again provides the key to understanding the general problem of the destruction of vorticity by viscosity near to the origin in general smooth flows. Finally § 6 offers a concluding discussion.

## 2. Passive scalar: an exact solution

Using plane polar coordinates $(r, \theta)$, a passive scalar $\Sigma(r, \theta, t)$ in the incompressible flow $\boldsymbol{u} = r^{-1}\partial_\theta \Psi\, \hat{\boldsymbol{r}} - \partial_r \Psi\, \hat{\boldsymbol{\theta}}$ given by the stream function $\Psi$ obeys the equation

$$\partial_t \Sigma + J(\Sigma, \Psi) = \varepsilon \nabla^2 \Sigma \quad (\varepsilon \equiv P^{-1}), \tag{2.1}$$

with

$$J(a, b) \equiv r^{-1}(\partial_r a\, \partial_\theta b - \partial_\theta a\, \partial_r b) \tag{2.2}$$

(e.g. Rhines & Young 1983). This equation is non-dimensionalized using the scale of the flow and its turn-over time, and we are interested in the limit of weak diffusion and large Péclet number $\varepsilon = P^{-1} \to 0$. We consider the case of a smooth steady axisymmetric flow field $\Psi = \Psi(r)$, with angular velocity $\alpha(r) = -r^{-1}\partial_r \Psi$. We may take a Fourier mode

$$\Sigma(r, \theta, t) = \sigma(r, t)\mathrm{e}^{\mathrm{i}n\theta} + \text{c.c.} \quad (n \geqslant 1), \tag{2.3}$$

where 'c.c.' denotes the complex conjugate of the preceding expression. We do not consider the case $n = 0$, for which the shear–diffuse mechanism does not operate: distributions of scalar constant on streamlines decay only on the long $O(P)$ time scale (see Rhines & Young 1983). The most important case for a scalar is $n = 1$, which includes the case of an initially uniform gradient of scalar across the system; the effect of accelerated diffusion will be to homogenize the value of scalar within the closed streamlines.

The scalar field $\sigma$ evolves according to

$$\partial_t \sigma + \mathrm{i}n\alpha(r)\sigma = \varepsilon \Delta \sigma, \quad \Delta \equiv \partial_r^2 + r^{-1}\partial_r - n^2 r^{-2}. \tag{2.4}$$

In any smooth axisymmetric flow field the stream function $\Psi(r)$ must expand near

the origin as a power series in $r^2$, and so must the angular velocity $\alpha(r)$, defined by $\alpha(r) = -r^{-1}\partial_r \Psi$. The simplest non-trivial exact model to consider has

$$\alpha(r) = \alpha_0 + \alpha_1 r^2 \quad (\alpha_1 \neq 0). \tag{2.5}$$

The first term gives an unimportant solid-body rotation, while the second is the first allowed term giving differential rotation and so spiral wind-up and accelerated diffusion. The angular velocity here increases without bound as $r$ increases; however this unphysical feature will be rectified in the matched solutions of the next section.

We assume that the passive scalar field is everywhere smooth and so must tend to zero as $\sigma = O(r^n)$ at the origin. In the exact solution we consider the simplest allowable initial condition

$$\sigma(r, 0) \equiv \sigma_0(r) = cr^n, \tag{2.6}$$

where $c$ is a constant; for $n = 1$ this is precisely the case of a uniform scalar gradient. If there is no diffusion, $\varepsilon = 0$, then the solution of (2.4) for this initial condition is

$$\sigma = cr^n \mathrm{e}^{-\mathrm{i}n(\alpha_0 + \alpha_1 r^2)t} \quad (\varepsilon = 0), \tag{2.7}$$

which gives spiral wind-up and indefinite fine-scaling of the scalar field. With diffusion, $\varepsilon > 0$, we seek a solution of the form

$$\sigma = g(t) r^n \mathrm{e}^{-\mathrm{i}n\alpha_0 t - \mathrm{i}f(t)r^2} \tag{2.8}$$

(see Lighthill 1966; Brunet & Haynes 1995). Substituting this into equation (2.4) and equating terms in $\sigma$ and $r^2\sigma$ leads to two first-order differential equations

$$f' = n\alpha_1 - 4\mathrm{i}\varepsilon f^2, \quad g'/g = -4\mathrm{i}\varepsilon(n+1)f, \tag{2.9a,b}$$

which may be solved as

$$f(t) = n\alpha_1 \mu^{-1} \tanh\tau, \quad g(t) = c(\cosh\tau)^{-n-1}, \tag{2.10a,b}$$

with

$$\tau = \mu t, \quad \mu = (1+\mathrm{i})\sqrt{2\varepsilon n\alpha_1}. \tag{2.11}$$

Equations (2.8), (2.10) and (2.11) furnish an exact solution to the passive scalar problem defined by the sytem (2.4)–(2.6). It is helpful to think of $n\alpha_1 > 0$, but the results are also valid for $n\alpha_1 < 0$. Note that as $\varepsilon \to 0$ for fixed time $t$, this solution tends to the diffusionless solution (2.7) as $\mu^{-1}\tanh\tau \to t$.

The form of this solution is the key to the remainder of this paper, and it is worth interpreting carefully. We have in mind the case of low diffusivity, with $0 < \varepsilon \ll 1$ fixed, and we have to understand the solution as a function of radius $r$ at all times $t$. The situation is summarized schematically in figure 1 as a space–time diagram with axes $r$ and $t$. Plots of the scalar field $\Sigma(r, \theta, t)$ are also shown for three characteristic times in figures 2(*a–c*) for $n = 1$ and (*d–f*) for $n = 2$. Figures 2(*a, d*) show spiral wind-up occurring; (*b, e*) show the wave of accelerated diffusion approaching the origin, while (*c, f*) show what is left behind, an exponentially decaying eigenfunction of fixed form. Another view of the process is given by plotting the maximum value of the scalar field $\Sigma_{\max}(t)$ and its radial location $r_{\max}(t)$, given by

$$r_{\max}^2 = (\chi/\alpha_1)(\cosh 2\chi t + \cos 2\chi t)(\sinh 2\chi t - \sin 2\chi t)^{-1}, \tag{2.12a}$$

$$\Sigma_{\max}^2 = 8|c|^2(2\chi/\alpha_1 e)^n(\cosh 2\chi t + \cos 2\chi t)^{-1}(\sinh 2\chi t - \sin 2\chi t)^{-n}, \tag{2.12b}$$

where $\chi = \mathrm{Re}\ \mu$. Figure 3 shows $r_{\max}$ and $\Sigma_{\max}$ plotted against $t$ on a log–log scale, for $n = 1$ (solid) and $n = 2$ (dashed). There are two phases: in the first $r_{\max}$ and $\Sigma_{\max}$

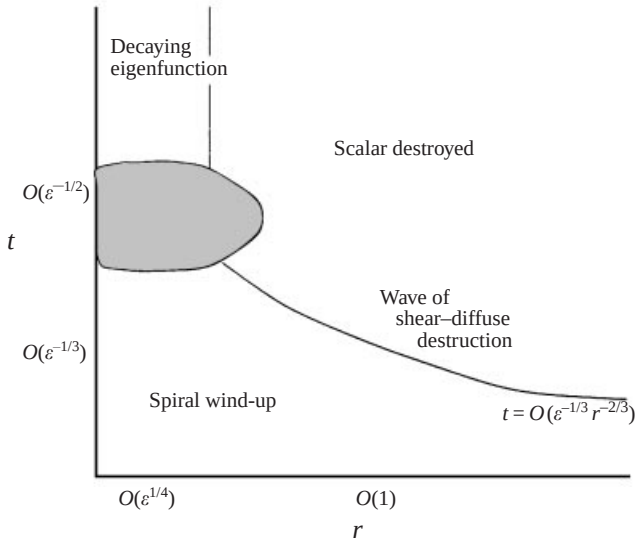


FIGURE 1. Schematic diagram of the evolution of a passive scalar. Different regimes are shown on a space–time diagram with axes $(r, t)$.

decrease algebraically with time, while in the second $r_{\max}$ equilibrates at a low level and $\Sigma_{\max}$ decreases faster, actually exponentially with time.

Plainly there are two important ranges of time, during which different processes occur. The first is $t \ll \varepsilon^{-1/2}$, corresponding to $\tau \ll 1$. We may then approximate (2.10) to give

$$f = n\alpha_1 t - 4\mathrm{i}n^2\alpha_1^2\varepsilon t^3/3 + O(\varepsilon^2 t^5), \quad g \sim c, \tag{2.13a,b}$$

and the leading approximation† for $\sigma$ is

$$\sigma(r,t) \sim cr^n \mathrm{e}^{-\mathrm{i}n(\alpha_0+\alpha_1 r^2)t}\, \mathrm{e}^{-4n^2\alpha_1^2 r^2 \varepsilon t^3/3}. \tag{2.14}$$

This shows the shear–diffuse mechanism (Moffatt & Kamkar 1983; Rhines & Young 1983): the second exponential term represents a decay superposed on the spiral wind-up in the first term. It is helpful to think informally of a 'wave' of shear–diffuse destruction approaching the origin from $r = \infty$, along the curve $t = O(\varepsilon^{-1/3} r^{-2/3})$ shown in figure 1: below this curve there is just spiral wind-up, above it the scalar is destroyed. This incoming wave can be seen in the plots, figure 2$(b, e)$, of the exact solution, and in figure 3.

The approximation (2.14) breaks down for $\tau = O(1)$, that is $t = O(\varepsilon^{-1/2})$, when the wave is a distance $r = O(\varepsilon^{1/4})$ from the origin. In this case all terms in the exact solution are important and govern evolution of the scalar in the shaded region of figure 1; this corresponds to the cross-over between the two phases visible in figure 3. For larger times $t \gg \varepsilon^{-1/2}$ and $\tau \gg 1$ we may again approximate

$$f(t) \sim n\alpha_1/\mu, \quad g(t) \sim c2^{n+1}\mathrm{e}^{-(n+1)\mu t}, \tag{2.15a,b}$$

which leads to

$$\sigma(r,t) \sim cr^n\, 2^{n+1}\, \mathrm{e}^{-n\alpha_1 r^2/\mu}\, \mathrm{e}^{pt}, \quad p = -\mathrm{i}n\alpha_0 - (n+1)\mu. \tag{2.16}$$

† Strictly the approximation is only valid for $t \ll \varepsilon^{-2/5}$. If more terms are retained in $f$ the period of validity increases and approaches $t = O(\varepsilon^{-1/2})$, when the whole expansion becomes non-uniform.

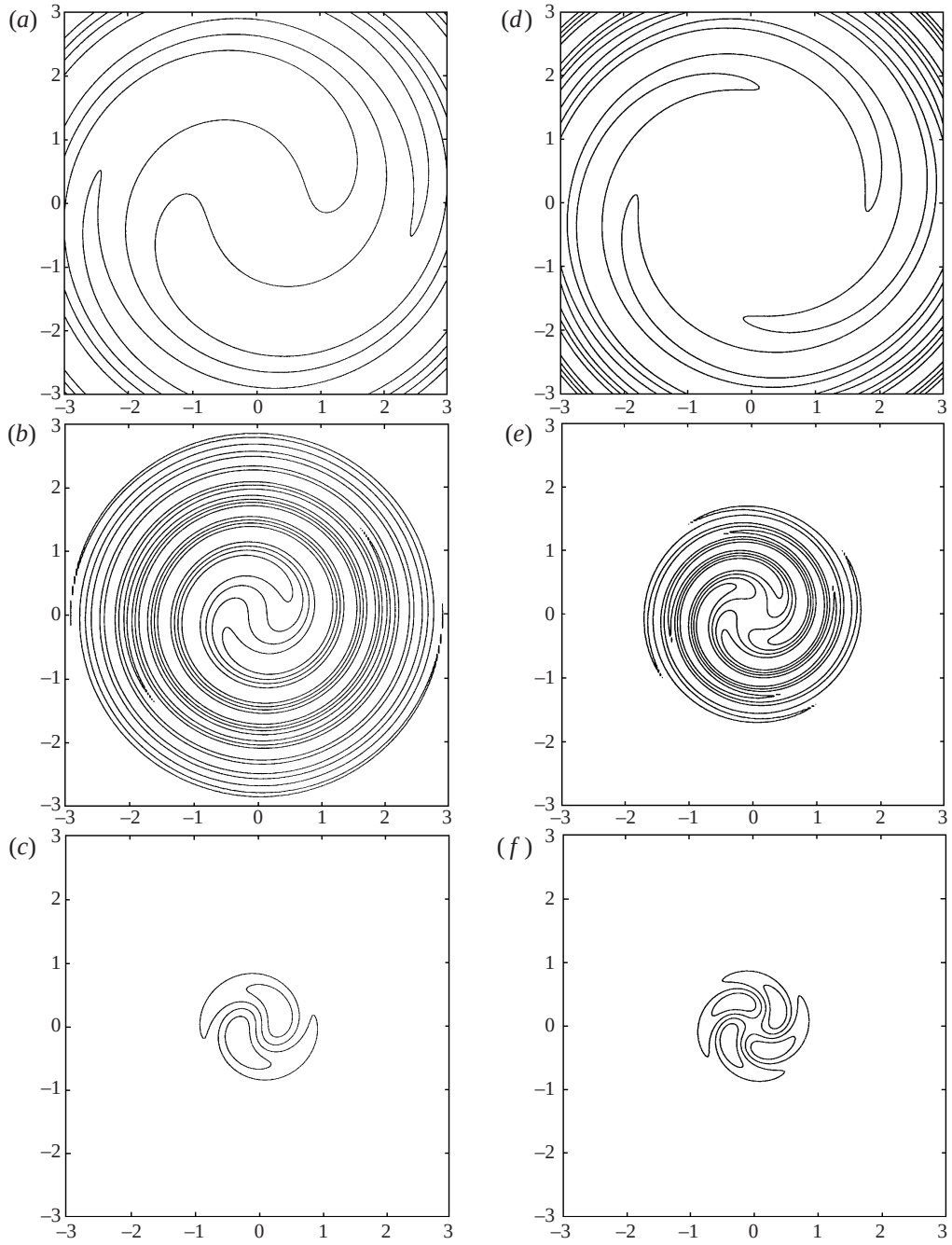


FIGURE 2. Evolution of isolines of a passive scalar $\Sigma(r,\theta,t)$ as given by the exact solution (2.8), (2.10) and (2.11), for $(a,c)$ $t=0.5$, $(b,d)$ $t=3$, and $(c,f)$ $t=20$. In $(a$–$c)$ $n=1$, while in $(d$–$f)$ $n=2$. Other parameter values are $c=1$, $\alpha_0=0$, $\alpha_1=1$ and $\varepsilon=0.01$.

This asymptotic solution represents a decaying, rotating eigenfunction with a Gaussian structure, seen in figure 2$(c,f)$ and in figure 3.

It decays exponentially on the $t=O(\varepsilon^{-1/2})$ time scale since

$$\mathrm{Re}\ p=-(n+1)\sqrt{2\varepsilon n\alpha_1}. \tag{2.17}$$

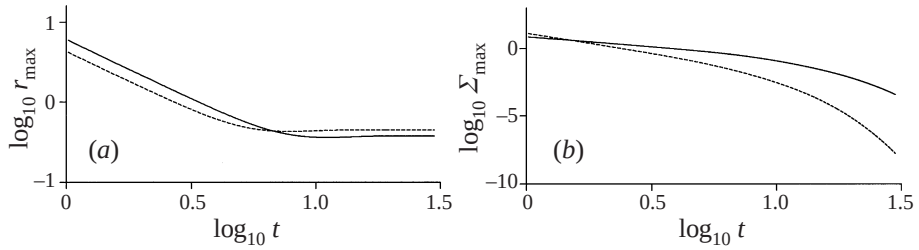


FIGURE 3. Plot of (*a*) $\log_{10} r_{\max}$ as a function of $\log_{10} t$, and (*b*) $\log_{10} \Sigma_{\max}$ as a function of $\log_{10} t$. Parameter values are as in figure 2 with the $n = 1$ curve solid and $n = 2$ dashed.

This is slower than the $O(\varepsilon^{-1/3})$ shear–diffuse time scale, but faster than the long $O(\varepsilon^{-1})$ time scale of molecular diffusion because the residual differential rotation at the origin enhances diffusion by reducing the radial scale to $r = O(\varepsilon^{1/4})$. This longer time scale is a result of the 'survival' of the vorticity at the vortex centre. At $t = O(\varepsilon^{-1/2})$, when we see a clear transition from algebraic to exponential decay in figure 3(*b*), the amplitude of the solution is already quite low, with $\Sigma_{\max} = O(\varepsilon^{n/4})$. A more precise estimate may be obtained from figure 3(*a*) using (2.12). In the first phase $r_{\max}$ decays according to $r_{\max}^2 \sim 3/(4\alpha_1\chi^2 t^3)$ while in the second phase $r_{\max}$ equilibrates at $r_{\max}^2 \sim \chi/\alpha_1$. Equating these two approximations for $r_{\max}$ gives the time of the cross-over, when

$$t \sim (3/4)^{1/3}\chi^{-1} \equiv (3/4)^{1/3}(2\varepsilon n\alpha_1)^{-1/2}, \quad \Sigma_{\max} \simeq 1.66|c|(0.264\varepsilon n/\alpha_1)^{n/4}. \tag{2.18}$$

We shall generalize and elaborate on this basic example in the following sections. However it enables us to answer the question of the time scale for destruction of the scalar at the centre of the vortex. This time scale is $O(P^{1/2})$, longer than the shear–diffuse $O(P^{1/3})$ time scale for radii where $\alpha'(r)$ does not vanish.

## 3. Passive scalar: the general case

The case of a passive scalar in a general smooth axisymmetric flow field becomes straightforward given the exact solution in § 2. Assuming smoothness of the flow field and of the passive scalar, we now have

$$\alpha(r) = \alpha_0 + \alpha_1 r^2 + O(r^4) \quad (\alpha_1 \neq 0), \tag{3.1}$$

$$\sigma(r, 0) = \sigma_0(r) = cr^n + O(r^{n+2}), \tag{3.2}$$

as $r \to 0$, in place of (2.5), (2.6). We assume that $\alpha'(r)$ is non-zero for $r > 0$.

The solution giving the wind-up and decay of scalar through the shear–diffuse mechanism takes the form

$$\sigma(r, t) \sim \sigma_0(r)\mathrm{e}^{-\mathrm{i}n\alpha(r)t}\mathrm{e}^{-n^2\alpha'(r)^2\varepsilon t^3/3} \tag{3.3}$$

for $r = O(1)$, as derived in Moffatt & Kamkar (1983) and Rhines & Young (1983). The accelerated decay of scalar strikes at the radius or radii where $|\alpha'(r)|$ is maximum and spreads out from there. For example, for an isolated Gaussian vortex, $\alpha'(r)$ has a single maximum and tends to zero as $r \to 0$ or $r \to \infty$. The decay of scalar spreads out towards the origin, and towards large radii. For the wave of shear–diffuse destruction which approaches $r = 0$ with increasing time, figure 1 once more becomes relevant. The solution (3.3) becomes invalid at $t = O(\varepsilon^{-1/2})$ (Moffatt & Kamkar 1983), at which point the wave has reached a radius $r = O(\varepsilon^{1/4})$.

This represents an inner region, and to find out what happens subsequently to the scalar at these distances from the origin (the scalar further out having already been destroyed), we introduce a short length scale $s$ and long time scale $T$ with $r = \varepsilon^{1/4}s$ and $t = \varepsilon^{-1/2}T$. We set

$$\sigma(r,t) = \mathrm{e}^{-\mathrm{i}n\alpha_0 t}\,[\rho(s,T) + O(\varepsilon^{1/2})], \tag{3.4}$$

taking out the angular velocity at the origin. The leading-order field $\rho$ satisfies

$$\partial_T \rho + \mathrm{i}n\alpha_1 s^2 \rho = (\partial_s^2 + s^{-1}\partial_s - n^2 s^{-2})\rho. \tag{3.5}$$

This is precisely the equation for the model problem of § 2 (see (2.4), (2.5)) with $\varepsilon = 1$ and $\alpha_0 = 0$. We can read off the solution for $\rho$ and rewrite this in terms of $t$, $r$ and $\varepsilon$ to obtain

$$\sigma(r,t) \sim g(t) r^n \mathrm{e}^{-\mathrm{i}n\alpha_0 t - \mathrm{i}f(t)r^2} \quad (0 \leqslant r \ll 1), \tag{3.6}$$

with $f$ and $g$ defined in (2.10), (2.11) above. This matches onto the solution (3.3) for moderate times, $t \ll \varepsilon^{-1/2}$, and for long times becomes precisely the decaying eigenfunction given above in (2.16). The errors in this approximation are of order $\varepsilon^{1/2}$.

In conclusion, the schematic diagram of figure 1 applies in the case of generic smooth flows with circular streamlines provided that the differential rotation vanishes nowhere except at the origin. The wave of shear–diffuse destruction approaching the origin arrives at a time of order $P^{1/2}$; on this time scale the scalar gradient there is destroyed according to the exact solution of § 2. Left behind is only an exponentially decaying remnant of the passive scalar field. If $\alpha'(r)$ also tends to zero as $r \to \infty$ then another wave heads outwards to large radii (Bernoff & Lingevitch 1994; Bajer 1998).

## 4. Magnetic field: flux expulsion

We consider briefly the problem of wind-up of magnetic field and flux expulsion. The field lies in the plane of the flow and we write $\boldsymbol{B} = \nabla \times (A\hat{\boldsymbol{z}})$. The component $A(r,\theta,t)$ of the magnetic vector potential is transported as a passive scalar with diffusivity $\varepsilon = {R_m}^{-1}$, where $R_m$ is the magnetic Reynolds number. The results of § 2 and § 3 now hold when $\Sigma$ is replaced by $A$, and analogously $\sigma$ by $a$. Isolines of the scalar field $\Sigma$ become isolines of $A$, and these are magnetic field lines. The evolution of these isolines shown in figure 2 may be interpreted in these new terms. The magnetic field is

$$\boldsymbol{B} \equiv \boldsymbol{b}(r,t)\mathrm{e}^{\mathrm{i}n\theta} + \text{c.c.}, \quad \boldsymbol{b}(r,t) = \mathrm{i}nar^{-1}\,\hat{\boldsymbol{r}} - \partial_r a\,\hat{\boldsymbol{\theta}}. \tag{4.1}$$

We shall focus on the specific case $n = 1$ (figure 2*a–c*), which is of primary importance as it includes the case of a uniform magnetic field crossing the region of closed streamlines, as in the simulations of Weiss (1966). The first phase of differential rotation and shear–diffuse destruction for the vector potential yields a magnetic field

$$\boldsymbol{b} \sim [\mathrm{i}a_0 r^{-1}\,\hat{\boldsymbol{r}} - (a_0' - a_0(\mathrm{i}\alpha' t + 2\alpha'\alpha''\varepsilon t^3/3))\hat{\boldsymbol{\theta}}]\mathrm{e}^{-\mathrm{i}\alpha t}\mathrm{e}^{-\alpha'^2\varepsilon t^3/3} \quad (r = O(1)), \tag{4.2}$$

using the solution (3.3) for $a$, with initial condition $a(r,0) = a_0(r)$. At a radius of order unity fields grow to a strength $O(\varepsilon^{-1/3})$ before being damped by the shear–diffuse mechanism on the time scale $O(\varepsilon^{-1/3})$ as seen numerically (Weiss 1966). These maximum fields correspond to points on figure 1 for $r = O(1)$ lying just below the wave of shear–diffuse destruction. Note that as the field increases, so does the Lorentz force feedback on the flow. If $R_m$ is increased, the initial level of the field is ever more

tightly constrained if its evolution is to remain kinematic, not affecting the flow field, until eliminated by diffusion.

If we move in closer to the origin, following the shear–diffuse wave sketched in figure 1, the maximum fields decrease. It may be verified that as the shaded region ($r = O(\varepsilon^{1/4})$, $t = O(\varepsilon^{-1/2})$) is approached the maximum field tends to values of only order unity before being destroyed by diffusion. The field near the centre of the vortex behaves as

$$\boldsymbol{b} \sim g(t)[\mathrm{i}\hat{\boldsymbol{r}} - (1 - 2\mathrm{i}f(t)r^2)\hat{\boldsymbol{\theta}}]\mathrm{e}^{-\mathrm{i}\alpha_0 t - \mathrm{i}f(t)r^2} \quad (0 \leqslant r \ll 1) \tag{4.3}$$

from (3.6) and taking $a_0(r) \sim cr$ as $r \to 0$.

At the very centre, $r = 0$, we may substitute for $g(t)$ from (2.10*b*) and use (4.1) to obtain

$$\boldsymbol{B} \sim 2|c|\,[\cosh((1+\mathrm{i})t\sqrt{2\varepsilon\alpha_1})]^{-2}(\boldsymbol{i}\sin(\alpha_0 t - \phi) - \boldsymbol{j}\cos(\alpha_0 t - \phi)) \tag{4.4}$$

in terms of Cartesian unit vectors, with $c = |c|\mathrm{e}^{\mathrm{i}\phi}$. For $t \ll \varepsilon^{-1/2}$ the vector at the origin undergoes solid-body rotation, and then for $t \gg \varepsilon^{-1/2}$ decays exponentially according to this prescription, valid for general flow fields provided $\alpha_1 \neq 0$ at the origin. This relatively slow decay at the centre was noted by Weiss (1966); see his figure 6. If $\alpha_1 = 0$ the time scale will become longer: if $\alpha(r) \sim \alpha_0 + \alpha_m r^{2m}$ at leading order with $\alpha_m \neq 0$, then balancing the terms $\partial_t$, $\alpha_m r^{2m}$ and $\varepsilon\Delta$ indicates that the time scale for decay at the origin is $t = O(\varepsilon^{-2m/(2m+2)})$, and the spatial scale is $r = O(\varepsilon^{1/(2m+2)})$. In the extreme case of solid-body rotation near the origin the time scale of diffusion becomes of order $R_m$ (Parker 1966).

## 5. Vorticity: an exact solution

We now consider the evolution of weak vorticity in a steady flow with circular streamlines, having stream function $\Psi(r)$ and vorticity $\Omega(r) = -\nabla^2\Psi$. We shall not be concerned about how this flow is maintained; it could be driven by body forces, or by distant boundaries. Alternatively it could be decaying viscously on a long time scale, say $O(R)$, much longer than the processes described below. Weak vorticity $\omega(r,\theta,t)$, with corresponding stream function $\psi(r,\theta,t)$, is introduced into the flow and satisfies the linearized Navier–Stokes equation

$$\partial_t\omega + J(\omega,\Psi) + J(\Omega,\psi) = \varepsilon\nabla^2\omega, \quad \omega = -\nabla^2\psi \quad (\varepsilon \equiv R^{-1}), \tag{5.1}$$

where $R$ is the Reynolds number. Replacing $\omega(r,\theta,t)$ and $\psi(r,\theta,t)$ by Fourier modes $\omega(r,t)\mathrm{e}^{\mathrm{i}n\theta}$ and $\psi(r,t)\mathrm{e}^{\mathrm{i}n\theta}$ (using the same symbols to avoid introducing further notation) leads to the equations

$$\partial_t\omega + \mathrm{i}n\alpha(r)\omega + \mathrm{i}n\beta(r)\psi = \varepsilon\Delta\omega, \quad \omega = -\Delta\psi, \tag{5.2}$$

where the angular velocity $\alpha(r)$ and the vorticity gradient $r\beta(r)$ are given by

$$\alpha(r) = -r^{-1}\partial_r\Psi, \quad \beta(r) = r^{-1}\partial_r\Omega = r^{-1}\partial_r(r^{-1}\partial_r(r^2\alpha)) \tag{5.3}$$

in terms of the basic flow. We again exclude the case $n = 0$. The case $n = 2$ represents the leading vorticity fluctuations generated by straining a coherent vortex, for example in two-dimensional turbulence. The case $n = 1$ corresponds to the homogenization of a uniform vorticity gradient, a Poiseuille flow, by the vortex, but also includes the steady solutions corresponding to infinitesimal translations of the vortex, which do not undergo spiral wind-up (see Lingevitch & Bernoff 1995; Llewellyn Smith 1995).

We assume that spiral wind-up of vorticity occurs (see for example the 'mixing

hypothesis' of Bernoff & Lingevitch 1994), and seek an exact solution to the equation (5.2) that describes this process. Motivated by § 2, we take

$$\alpha(r) = \alpha_0 + \alpha_1 r^2, \quad \beta(r) = 8\alpha_1 \tag{5.4}$$

(using (5.3)). We then have to solve

$$\partial_t \omega + \mathrm{i}n(\alpha_0 + \alpha_1 r^2)\omega + 8\mathrm{i}n\alpha_1 \psi = \varepsilon \Delta \omega, \quad \omega = -\Delta \psi. \tag{5.5}$$

Noting that $\omega$, $\psi = O(r^n)$ at the origin, it is convenient to transform to $X$ and $Y$ given by

$$\omega = r^n \mathrm{e}^{-\mathrm{i}n\alpha_0 t} X(r,t), \quad \psi = r^n \mathrm{e}^{-\mathrm{i}n\alpha_0 t} Y(r,t) \tag{5.6}$$

so that the governing equations become

$$\partial_t X + \mathrm{i}n\alpha_1 r^2 X + 8\mathrm{i}n\alpha_1 Y = \varepsilon \Delta_1 X, \quad -X = \Delta_1 Y, \tag{5.7a,b}$$

with $\Delta_1 \equiv \partial_r^2 + (2n+1)r^{-1}\partial_r$.

If there is no viscosity, $\varepsilon = 0$, then an exact solution may be written in terms of Kummer functions (see Abramowitz & Stegun 1965, herein referred to as AS),

$$X = ct^{n/2-\kappa} M(a+1, b, s), \quad Y = dt^{n/2-\kappa-1} M(a,b,s), \quad s = -\mathrm{i}n\alpha_1 r^2 t, \tag{5.8}$$

where

$$\kappa = \frac{1}{2}\sqrt{n^2+8}, \quad a = \kappa + n/2, \quad b = n+1, \quad \frac{d}{c} = \frac{\kappa - n/2}{8\mathrm{i}n\alpha_1} \tag{5.9}$$

(BG). This solution represents spiral wind-up at some distance from the origin, matched onto a solution that is regular at the origin itself. Further discussion is given when viscosity is introduced below.

Now we seek an exact solution with viscosity using the *ansatz*

$$X = g(t) M(a+1, b, s), \quad Y = h(t) M(a,b,s), \quad s = -\mathrm{i}r^2 f(t), \tag{5.10}$$

with $a$ and $b$ defined above in (5.9). This *ansatz* is substituted into (5.7) and gives differential equations for $f(t)$, $g(t)$ and $h(t)$. Relegating the details to an Appendix, the resulting exact solution is given by

$$\omega = g(t) r^n \mathrm{e}^{-\mathrm{i}n\alpha_0 t} M(a+1,b,s), \quad \psi = h(t) r^n \mathrm{e}^{-\mathrm{i}n\alpha_0 t} M(a,b,s), \quad s = -\mathrm{i}r^2 f(t), \tag{5.11}$$

with

$$f(t) = n\alpha_1 \mu^{-1} \tanh \tau, \tag{5.12a}$$

$$g(t) = c(\mu^{-1} \sinh \tau)^{n/2-\kappa} (\cosh \tau)^{-n/2-\kappa-1}, \tag{5.12b}$$

$$h(t) = d(\mu^{-1} \sinh \tau)^{n/2-\kappa-1} (\cosh \tau)^{-n/2-\kappa}, \tag{5.12c}$$

$$\tau = \mu t, \quad \mu = (1+\mathrm{i})\sqrt{2\varepsilon n \alpha_1} \tag{5.12d}$$

and constants defined as in (5.9).

Equations (5.11), (5.12) are an exact solution to evolution under the viscous linearized Navier–Stokes equations (5.2), with the basic angular velocity profile given in (5.4). The function $f(t)$ and variable $\tau$ are the same as in the case of a passive scalar. Also note that $\mu^{-1} \sinh \tau \to t$ in the limit $\varepsilon \to 0$ and so the viscous solution (5.11), (5.12) reduces precisely to the inviscid solution (5.6), (5.8) in this limit.

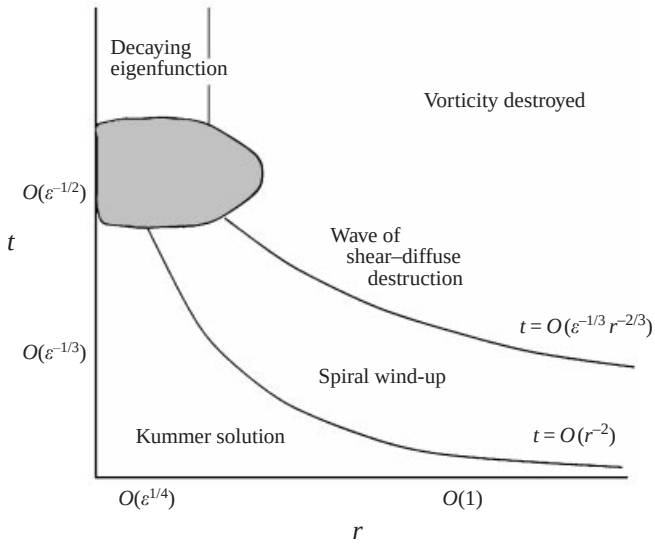


FIGURE 4. Schematic diagram of the evolution of weak vorticity. Different regimes are shown on a space–time diagram with axes $(r, t)$.

Figure 4 gives a schematic interpretation of behaviour of the solution in a space–time diagram, and figure 5 shows the exact solution at various times for $n = 1$ and $n = 2$. These two figures parallel the earlier figures 1 and 2 for the passive scalar. Note that for the case $n = 1$, the constants $\kappa = 3/2$, $a = 2$ and $b = 2$; the Kummer functions in (5.11) take the simple form

$$M(a, b, s) = \mathrm{e}^s, \quad M(a + 1, b, s) = (1 + s/2)\mathrm{e}^s$$

(AS 13.6.12, 13.4.10).

To understand the exact solutions plotted in figure 5, we first consider moderate times. In this case spiral wind-up occurs (figure 5*a*, *d*) and vorticity in outer regions is destroyed by the shear–diffuse mechanism (figure 5*b*, *e*). This is correct for $1 \ll t \ll \varepsilon^{-1/2}$, that is $\tau \ll 1$, and we may use the approximations

$$f = n\alpha_1 t - 4\mathrm{i}n^2\alpha_1^2\varepsilon t^3/3 + O(\varepsilon^2 t^5), \quad g \sim ct^{n/2-\kappa}, \quad h \sim dt^{n/2-\kappa-1}. \tag{5.13}$$

We substitute these into the exact solution. For small radii $r = O(t^{-1/2})$ the Kummer functions cannot be approximated, as $s$ is of order unity. In this case we are in the region marked 'Kummer solution' in figure 4; here the Kummer functions give an inner solution, regular at the origin, that matches onto the region labelled 'spiral wind-up' further away. In this region of spiral wind-up $r \gg t^{-1/2}$, implying $s \gg 1$, and we may approximate the Kummer functions using the formula

$$M(a, b, s) \sim \mathrm{e}^s s^{a-b}\Gamma(b)/\Gamma(a) \tag{5.14}$$

(AS 13.5.1). In this case the solution reduces to

$$\omega \sim Cr^{2\kappa}\mathrm{e}^{-\mathrm{i}n(\alpha_0+\alpha_1 r^2)t}\mathrm{e}^{-4n^2\alpha_1^2 r^2\varepsilon t^3/3}, \quad \psi \sim \omega(4n^2\alpha_1^2 r^2 t^2)^{-1}, \tag{5.15}$$

with $C = c(-\mathrm{i}n\alpha_1)^{\kappa-n/2}n!/\Gamma(\kappa + n/2 + 1)$. This gives spiral wind-up of vorticity with a $Cr^{2\kappa}$ envelope, together with a wave of shear–diffuse destruction approaching the origin at a distance $r = \varepsilon^{-1/2}t^{-3/2}$ (see figure 4).

At times $t = O(\varepsilon^{-1/2})$ the wave of destruction reaches radii of order $r = O(\varepsilon^{1/4})$

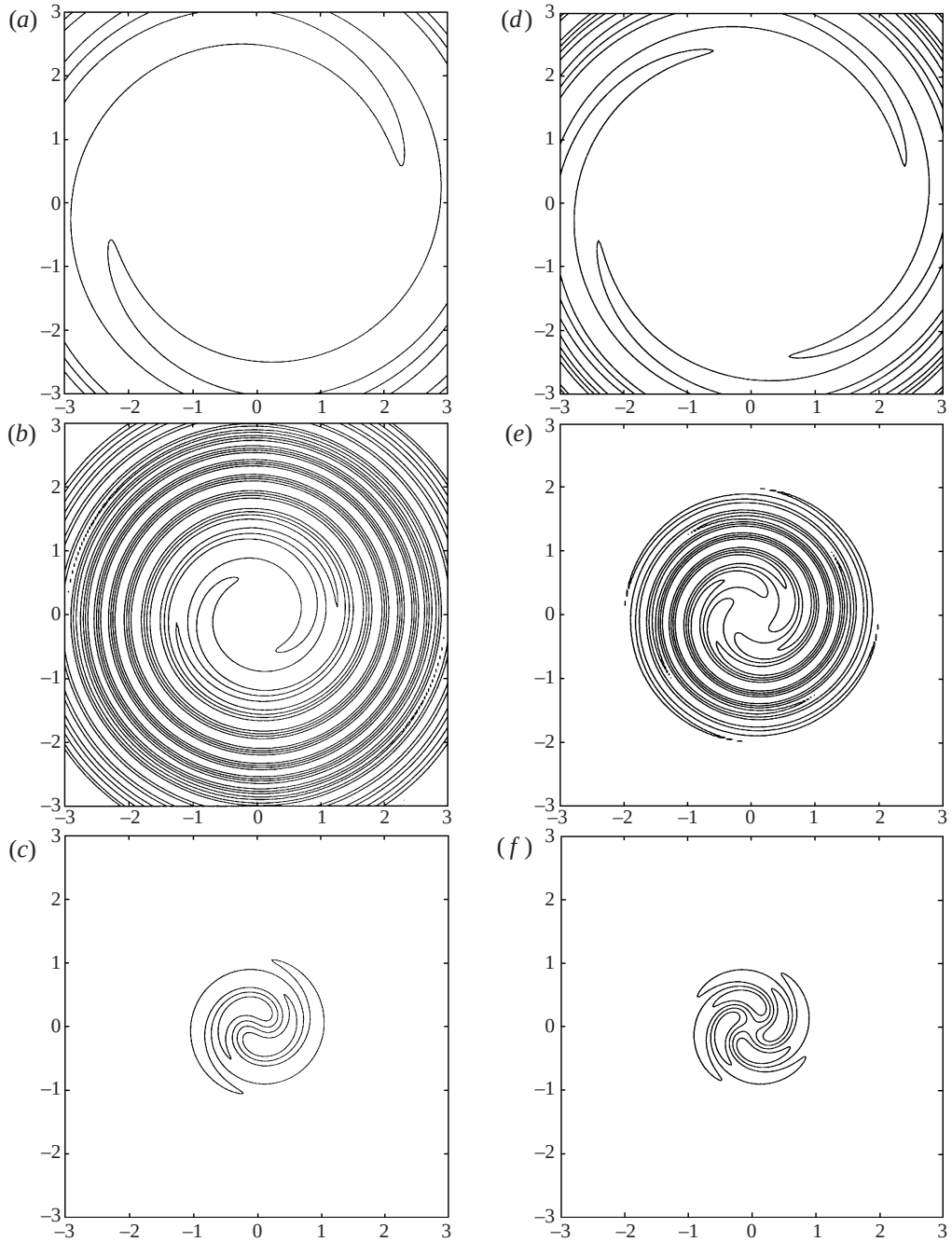


FIGURE 5. Evolution of isolines of weak vorticity $\omega(r, \theta, t)$ as given by the exact solution (5.11), (5.12). In (*a–c*) $n = 1$, while in (*d–f*) $n = 2$. Parameter values and times are as in figure 2.

from the origin and the above approximation breaks down; the boundary $r = O(t^{-1/2})$ between the inner Kummer function solution and the region of spiral wind-up also reaches these radii at these times, and all elements of the solution are involved in the shaded region of figure 4.

At later times $t \gg \varepsilon^{-1/2}$, that is $\tau \gg 1$, the vorticity field settles down to an exponentially decaying eigenfunction of constant spatial structure, as shown in figure 5($c, f$). To obtain its form analytically we again approximate, with

$$f \sim n\alpha_1/\mu, \quad g \sim c\mu^{\kappa-n/2}2^{2\kappa+1}\mathrm{e}^{-(2\kappa+1)\mu t}, \quad h \sim d\mu^{\kappa+1-n/2}2^{2\kappa+1}\mathrm{e}^{-(2\kappa+1)\mu t}, \tag{5.16}$$

to give

$$\omega \sim c\mu^{\kappa-n/2}r^n 2^{2\kappa+1}\mathrm{e}^{pt}M(a+1,b,s), \quad \psi \sim d\mu^{\kappa+1-n/2}r^n 2^{2\kappa+1}\mathrm{e}^{pt}M(a,b,s), \tag{5.17a}$$

$$s = -\mathrm{i}n\alpha_1 r^2/\mu, \quad p = -\mathrm{i}n\alpha_0 - (2\kappa+1)\mu. \tag{5.17b}$$

This represents an eigenfunction with decay rate

$$\mathrm{Re}\ p = -(2\kappa+1)\sqrt{2\varepsilon n\alpha_1} \equiv -(\sqrt{n^2+8}+1)\sqrt{2\varepsilon n\alpha_1}. \tag{5.18}$$

Note that the decay here is faster than in the scalar case (cf. (2.17)). The eigenfunction forms may be seen in figure 5($c, f$); although written in terms of Kummer functions these have similarities with the Gaussian forms for a passive scalar in figure 2($c, f$).

The exact solution for vorticity may again be used as an inner solution for wind-up in more general angular velocity profiles $\alpha(r)$, and in this case figure 4 continues to show the situation schematically. An approximate long-time solution capturing spiral wind-up and destruction by the shear–diffuse mechanism for general $\alpha(r)$ is given by

$$\omega \sim g(r)\mathrm{e}^{-\mathrm{i}n\alpha(r)t}\mathrm{e}^{-n^2\alpha'(r)^2\varepsilon t^3/3}, \quad \psi \sim \omega(n^2\alpha'(r)^2t^2)^{-1}, \tag{5.19}$$

valid for $r \gg t^{-1/2}$ (Lundgren 1982; Bernoff & Lingevitch 1994; BG). Here the vorticity is acting as a passive scalar at leading order, and the stream function is subdominant. The function $g$ has the scaling behaviour $g(r) \sim Cr^{2\kappa}$ for small $r$. Analogously to the discussion in § 3, if this full solution is approximated for small $r$, it gives that in (5.15), and so the exact solution (5.11) acts as an inner solution for (5.19); this includes satisfying regularity at the origin, and capturing the behaviour of the shear–diffuse wave as it comes inwards, in (5.19) and (5.15), to destroy the vorticity there on the $O(R^{1/2})$ time scale and leave only an exponentially decaying remnant, (5.17). This time scale has also been found by Prochazka & Pullin (1995) in an eigenvalue study of perturbations to a Gaussian vortex. However their eigenfunctions are localized near the edge of the vortex, whereas we focus on the centre of the vortex.

For vorticity the role of the exact solution as an inner solution is more fundamental than for the passive scalar. In the latter case, the exact solution corresponds to a definite initial condition (2.6). However for vorticity the exact solution (5.11), (5.12) diverges if we reduce $t$ to zero. This is a result of the active coupling of vorticity to the stream function and the unboundedness of $\alpha(r)$ for increasing $r$ in the exact solution. Conversely as time is increased this same coupling leads to a rather rapid suppression of vorticity near the origin with an emergent power law $g(r) \sim Cr^{2\kappa}$ that is fairly flat, even before diffusion takes hold. Let us consider a realistic situation, say a finite smooth vortex, for which the quadratic behaviour of $\alpha(r)$ only applies close to the origin, and introduce weak vorticity. There follows a transient for $t = O(1)$, during which none of the above theory applies, before spiral wind-up occurs for $t \gg 1$. The field is then described by Lundgren's (1982) solution (5.19), and the exact solution discussed in this section plays its role as an inner solution, describing inviscid suppression of vorticity close to the origin, and the subsequent damping effects of viscosity.

## 6. Discussion

We have analysed the cases of a passive scalar, magnetic field and weak vorticity by means of exact solutions that may be matched onto very general solutions for the wind-up and accelerated diffusion of these fields in circular streamlines. We find that while the time scales for accelerated diffusion by the shear–diffuse mechanism are $O(P^{1/3})$, $O({R_m}^{1/3})$ and $O(R^{1/3})$ respectively, these estimates become invalid near the centre of the streamlines. Fields there are only destroyed on the longer time scales $O(P^{1/2})$, $O({R_m}^{1/2})$ and $O(R^{1/2})$ respectively, to leave behind a vanishing remnant, an eigenfunction decaying exponentially.

The origin is significant as it corresponds to a point where $\alpha'(r) = 0$ and so a point where spiral wind-up occurs non-uniformly. A similar situation arises if this occurs at some non-zero radius, or if the flow field is such that $\alpha(r) \to 0$ as $r \to \infty$. For a localized vortex, this latter problem is equivalent to wind-up by a point vortex at the origin, and has been considered for vorticity by Bernoff & Lingevitch (1994) and magnetic fields by Bajer (1998); note that a passive scalar and weak vorticity behave analogously in the far field (as $\beta \simeq 0$ there).

A key assumption in our study is that the underlying flow is infinitely differentiable at the origin, which forces the behaviour $\alpha(r) \simeq \alpha_0 + \alpha_1 r^2$ for small $r$. However, non-smooth profiles have been set up in recent plasma physics experiments which correspond to vortices with $\alpha(r) \simeq \alpha_0 + \alpha_1 r$ (Driscoll & Fine 1990; Cass 1998; Schecter *et al.* 1999, 2000). This profile is singular as $\nabla^2\Omega \simeq 3\alpha_1/r$ and so in the presence of viscosity the profile would be smoothed out, at least on some fine, inner length scale. Extending our work to this case remains a topic for further investigation; here we only note that the length and time scales for decay at the origin are given by $r = O(\varepsilon^{1/3})$ and $t = O(\varepsilon^{-1/3})$. We have also assumed that the underlying flow with circular streamlines is steady. Essentially it can only evolve on a time scale longer than $O(P^{1/2})$, $O({R_m}^{1/2})$ or $O(R^{1/2})$, respectively. If the vortex is decaying freely through viscosity then it will evolve on an $O(R)$ time scale, and so for the analysis we have presented to be valid for a passive scalar we require $P \ll R^2$, and $R_m \ll R^2$ for magnetic field. Otherwise the evolution of the underlying flow field would become involved in the problem.

This study could be extended in a number of ways. We have considered only circular streamlines and vortices where the flow lies in the plane. However vortices subject to two-dimensional strain (Jiménez *et al.* 1996; Bassom & Gilbert 1999) or three-dimensional strain, whether axisymmetric (Lundgren 1982) or not (Moffatt, Kida & Ohkitani 1994), are important in modelling turbulent flows in two and three dimensions. The basic shear–diffuse mechanism will undoubtedly be present in all these situations. Similar results would be expected for the case of a vortex in two-dimensional strain, replacing circular streamlines by ones of more general shape, locally elliptical at the origin. For the model of Lundgren (1982), the shear–diffuse mechanism is accelerated by axisymmetric stretching and occurs at times of order $\log R$. However, the situation is less clear for a vortex in three-dimensional non-axisymmetric strain (Moffatt *et al.* 1994) and this deserves further investigation. Finally note that from a mathematical point of view this class of problems is interesting because the advection–diffusion operator is non-normal with respect to an $L^2$ norm (see e.g. Trefethen 1997, example 5), and becomes increasingly so in the limit of weak diffusion; this allows long non-trivial transients, for example growing magnetic fields, before inevitable diffusive decay (see also Childress & Gilbert 1995, § 9.3.2, § 9.4).

We thank Professor Nigel Weiss for valuable comments on a draft manuscript. We are grateful to Professor Peter Haynes for sending us reprints and preprints, and to the referees and Dr Stephen Cowley for helpful comments and additional references. This work was supported by the British/Polish Joint Research Collaboration Programme of the British Council and the Komitet Badań Naukowych (KBN). A.G. would like to thank staff of the Institute of Geophysics of Warsaw University for their hospitality, and likewise K.B. the staff of the School of Mathematical Sciences of the University of Exeter. K.B. acknowledges further support from the KBN under grant number 2 P03B 13517. This paper was finalized at the Isaac Newton Institute, and A.G. and K.B. would like to thank the organisers of the 'Geometry and Topology of Fluid Flow' programme for inviting them to participate.

## Appendix

In this Appendix we indicate how the solutions (5.12) are obtained. Note that equations (5.9) fix the constants $\kappa$, $a$, $b$ and $d/c$ and imply the useful identity $a(\kappa - n/2) = 2$: we use these definitions repeatedly below without further comment. It may be checked that

$$\Delta_1 M(a, n+1, s) = -4\mathrm{i}af M(a+1, n+1, s) \tag{A 1}$$

for any $a$ (using AS 13.1.1, 13.4.10), and so (5.7$b$) requires

$$g = 4\mathrm{i}afh. \tag{A 2}$$

To satisfy (5.7$a$) we substitute (5.10) and use (A 1) to simplify the right-hand side, to yield

$$g'M(a+1,b,s) - \mathrm{i}r^2 f'gM'(a+1,b,s) + \mathrm{i}n\alpha_1 r^2 gM(a+1,b,s) \\ +8\mathrm{i}n\alpha_1 hM(a,b,s) = -4\mathrm{i}\varepsilon(a+1)fgM(a+2,b,s). \tag{A 3}$$

Replacing $r^2$ by $s$ using (5.10) and gathering some terms gives

$$(g' - n\alpha_1 sg/f)M(a+1,b,s) + (sgf'/f)M'(a+1,b,s) \\ +8\mathrm{i}n\alpha_1 hM(a,b,s) = -4\mathrm{i}\varepsilon(a+1)fgM(a+2,b,s). \tag{A 4}$$

Now we may use Kummer function identities to write this equation in terms only of $M(a+1,b,s)$ and $M'(a+1,b,s)$. Specifically, we have from AS 13.4.11, AS 13.4.10,

$$(n/2-\kappa)M(a,b,s) = (n/2-\kappa-s)M(a+1,b,s) + sM'(a+1,b,s), \tag{A 5}$$

$$(n/2+\kappa+1)M(a+2,b,s) = (n/2+\kappa+1)M(a+1,b,s) + sM'(a+1,b,s). \tag{A 6}$$

We substitute these into (A 4) to obtain a complicated expression. Nonetheless in terms of functions of $s$ it only involves the three independent terms $M(a+1,b,s)$, $sM(a+1,b,s)$ and $sM'(a+1,b,s)$. If we set the sum of terms multiplying each of these functions to zero we obtain three relations between functions of $t$, respectively,

$$g' + 8\mathrm{i}n\alpha_1 h = -4\mathrm{i}\varepsilon(\kappa + n/2 + 1)fg, \tag{A 7$a$}$$

$$-\frac{n\alpha_1 g}{f} + \frac{8\mathrm{i}n\alpha_1 h}{\kappa - n/2} = 0, \quad \frac{gf'}{f} - \frac{8\mathrm{i}n\alpha_1 h}{\kappa - n/2} = -4\mathrm{i}\varepsilon fg. \tag{A 7$b,c$}$$

The second of these is identically satisfied using (A 2). For the remaining two equations

we use (A 2) to eliminate $h$ and leave

$$g'/g = -n\alpha_1(\kappa - n/2)f^{-1} - 4\mathrm{i}\varepsilon(\kappa + n/2 + 1)f, \quad f' = n\alpha_1 - 4\mathrm{i}\varepsilon f^2. \qquad (\mathrm{A}\,8a,b)$$

Equation (A 8$b$) is the same as in the passive scalar case (see (2.9$a$)); given its solution (2.10$a$), (2.11), equation (A 8$a$) may be solved for $g$ and finally $h$ obtained from (A 2).

## REFERENCES


Abramowitz, M. & Stegun, I. A. 1965 *Handbook of Mathematical Functions*. Dover (referred to as AS herein).

Bajer, K. 1998 Flux expulsion by a point vortex. *Eur. J. Mech.* B/*Fluids* **17**, 653–664.

Bassom, A. P. & Gilbert, A. D. 1998 The spiral wind-up of vorticity in an inviscid planar vortex. *J. Fluid Mech.* **371**, 109–140 (referred to as BG herein).

Bassom, A. P. & Gilbert, A. D. 1999 The spiral wind-up and dissipation of vorticity and a passive scalar in a strained planar vortex. *J. Fluid Mech.* **398**, 245–270.

Bassom, A. P. & Gilbert, A. D. 2000 The relaxation of vorticity fluctuations in approximately elliptical streamlines. *Proc. R. Soc. Lond.* A **456**, 295–314.

Batchelor, G. K. 1956 Steady laminar flow with closed streamlines at large Reynolds number. *J. Fluid Mech.* **1**, 177–190.

Bernoff, A. J. & Lingevitch, J. F. 1994 Rapid relaxation of an axisymmetric vortex. *Phys. Fluids* **6**, 3717–3723.

Brunet, G. & Haynes, P. H. 1995 The nonlinear evolution of disturbances to a parabolic jet. *J. Atmos. Sci.* **52**, 464–477.

Cass, A. C. 1998 Experiments on vortex symmetrization in magnetized electron plasma columns. PhD Thesis, University of California at San Diego.

Childress, S. & Gilbert, A. D. 1995 *Stretch, Twist, Fold: The Fast Dynamo*. Springer.

Driscoll, C. F. & Fine, K. S. 1990 Experiments on vortex dynamics in pure electron plasmas. *Phys. Fluids* B **2**, 1359–1366.

Dritschel, D. G. 1998 On the persistence of non-axisymmetric vortices in inviscid two-dimensional flows. *J. Fluid Mech.* **371**, 141–155.

Flohr, P. & Vassilicos, J. C. 1997 Accelerated scalar dissipation in a vortex. *J. Fluid Mech.* **348**, 295–317.

Jiménez, J., Moffatt, H. K. & Vasco, C. 1996 The structure of vortices in freely decaying two-dimensional turbulence. *J. Fluid Mech.* **313**, 209–222.

Koumoutsakos, P. 1997 Inviscid axisymmetrization of an elliptical vortex. *J. Comput. Phys.* **138**, 821–857.

Lighthill, M. J. 1966 Initial development of diffusion in a Poiseuille flow. *J. Inst. Maths. Applics.* **2**, 97–108.

Lingevitch, J. F. & Bernoff, A. J. 1995 Distortion and evolution of a localized vortex in an irrotational flow. *Phys. Fluids* **7**, 1015–1026.

Llewellyn Smith, S. G. 1995 The influence of circulation on the stability of vortices to mode-one disturbances. *Proc. R. Soc. Lond.* A **451**, 747–755.

Lundgren, T. S. 1982 Strained spiral vortex model for turbulent fine structure. *Phys. Fluids* **25**, 2193–2203.

McCalpin, J. D. 1987 On the adjustment of azimuthally perturbed vortices. *J. Geophys. Res.* C **92**, 8213–8225.

Melander, M. V., McWilliams, J. C. & Zabusky, N. J. 1987 Axisymmetrization and vorticity-gradient intensification of an isolated two-dimensional vortex through filamentation. *J. Fluid Mech.* **178**, 137–159.

Moffatt, H. K. 1983 Transport effects associated with turbulence with particular attention to the influence of helicity. *Rep. Prog. Phys.* **46**, 621–664.

Moffatt, H. K. & Kamkar, H. 1983 On the time-scale associated with flux expulsion. In *Stellar and Planetary Magnetism* (ed. A. M. Soward), pp. 91–97. Gordon & Breach.

Moffatt, H. K., Kida, S. & Ohkitani, K. 1994 Stretched vortices – the sinews of turbulence: high Reynolds number asymptotics. *J. Fluid Mech.* **259**, 241–264.

PARKER, R. L. 1966 Reconnexion of lines of force in rotating spheres and cylinders. *Proc. R. Soc. Lond.* A **291**, 60–72.

PROCHAZKA, A. & PULLIN, D. I. 1995 On the two-dimensional stability of the axisymmetric Burgers vortex. *Phys. Fluids* **7**, 1788–1790.

RHINES, P. B. & YOUNG, W. R. 1982 Homogenization of potential vorticity in planetary gyres. *J. Fluid Mech.* **122**, 347–367.

RHINES, P. B. & YOUNG, W. R. 1983 How rapidly is a passive scalar mixed within closed streamlines? *J. Fluid Mech.* **133**, 133–145.

ROSSI, L. F., LINGEVITCH, J. F. & BERNOFF, A. J. 1997 Quasi-steady monopole and tripole attractors for relaxing vortices. *Phys. Fluids* **9**, 2329–2338.

SCHECTER, D. A., DUBIN, D. H. E., CASS, A. C., DRISCOLL, C. F., LANSKY, I. M. & O'NEIL, T. M. 1999 Inviscid damping of elliptical perturbations on a 2D vortex. In *Non-Neutral Plasma Physics III* (ed. J. J. Bollinger, R. L. Spencer & R. C. Davidson), pp. 115–122. AIP Press.

SCHECTER, D. A., DUBIN, D. H. E., CASS, A. C., DRISCOLL, C. F., LANSKY, I. M. & O'NEIL, T. M. 2000 Inviscid damping of asymmetries on a 2-d vortex. *Phys. Fluids* **12**, 2397–2412.

SMITH, G. B. & MONTGOMERY, M. T. 1995 Vortex axisymmetrization: dependence on azimuthal wave-number or asymmetric radial structure changes. *Q. J. R. Met. Soc.* **121**, 1615–1650.

STEWARTSON, K. 1978 The evolution of the critical layer of a Rossby wave. *Geophys. Astrophys. Fluid Dyn.* **9**, 185–200.

SUTYRIN, G. G. 1989 Azimuthal waves and symmetrization of an intense vortex. *Sov. Phys. Dokl.* **34**, 104–106.

TREFETHEN, L. N. 1997 Pseudospectra of linear operators. *SIAM Rev.* **39**, 383–406.

WEISS, N. O. 1966 The expulsion of magnetic flux by eddies. *Proc. R. Soc. Lond.* A **293**, 310–328.